

A Computational Analysis of Jet Vanes Thrust Vector Control for Solid Rocket Propulsion

Sameer Sheth*, Jacob Buell†, Noah Kraus‡, Atharva Gujrathi§, Hyeonbi Jee¶, Joshua Hammond||, Taekyung Kim**
Georgia Institute of Technology, Atlanta, Georgia, 30332

Thrust vector control (TVC) is an effective method of achieving active stability in rockets. Jet vane thrust vector control (JVTVC) systems are the most effective for many solid rocketry projects due to their ability to control pitch, roll, and yaw while also being considerably easier to manufacture compared to alternative TVC methods. Jet vanes are small fins positioned in the rocket motor's exhaust, redirecting the direction of the exhaust gas. To characterize the flow effects on and by the jet vanes, the GNC project under the Ramblin' Rocket Club at the Georgia Institute of Technology (GT) used the computational fluid dynamics (CFD) software Ansys Fluent. A model was created using supersonic, turbulent, and high-temperature flow conditions to analyze three jet vane design considerations: the vane geometry and material, heat transfer and erosion analysis on the vanes, and the overall thrust loss due to the vanes. This paper describes the assumptions, set-up, refinement, and results of the Ansys Fluent simulations. Lastly, this paper serves as a base model for collegiate engineering teams across the United States who wish to improve their comprehension of thrust vectoring propulsion systems and apply it to their engineering challenges.

I. Nomenclature

A	=	exit area
\dot{m}	=	mass flow rate
M	=	mach number
p	=	static pressure
p_t	=	total pressure
P	=	exit pressure
P_a	=	ambient pressure
T_{true}	=	True Thrust (neglecting reduction due to jet vanes)
T_{vanes}	=	Thrust (accounting for reduction jet vanes)
v	=	exit velocity
γ	=	ratio of specific heats
ρ	=	density

II. Introduction and Background

TVC is a system through which rockets may achieve active stability, by which the rocket detects and corrects deviations in its attitude and flight path. This system is distinct from passive stabilization, in which directional stability is typically achieved through aerodynamic effects. TVC reorients the direction of the thrust, providing the necessary moments on the rocket to align its flight path. TVC is preferable to passive stability for rockets flying in low airspeed flow regimes and upper atmospheric flight where the air is too thin for fins to achieve adequate restoring forces for stability. By varying their angle of attack, jet vanes can produce a wide range of side forces on the rocket, up to about

*Undergraduate Member, GT Ramblin' Rocket Club, Daniel Guggenheim School of Aerospace Engineering, AIAA Student Member 1603262

†Undergraduate Member, GT Ramblin' Rocket Club, Daniel Guggenheim School of Aerospace Engineering, AIAA Student Member 1538020

‡Undergraduate Member, GT Ramblin' Rocket Club, Daniel Guggenheim School of Aerospace Engineering, AIAA Student Member 603464

§Undergraduate Member, GT Ramblin' Rocket Club, Daniel Guggenheim School of Aerospace Engineering, AIAA Student Member 1603265

¶Undergraduate Member, GT Ramblin' Rocket Club, Daniel Guggenheim School of Aerospace Engineering, AIAA Student Member 1584153

||Undergraduate Member, GT Ramblin' Rocket Club, Daniel Guggenheim School of Aerospace Engineering, AIAA Student Member 1422732

**Undergraduate Member, GT Ramblin' Rocket Club, Daniel Guggenheim School of Aerospace Engineering, AIAA Student Member 1603498

6% of the rocket's thrust ([1]). An overall reduction in axial thrust occurs due to the drag caused by the jet vanes. Their direct exposure to extreme thermal and flow conditions presents a challenge in material selection and fluid dynamics ([2]). For most pure metals and alloys, the impact angle of maximum wear from erosion is approximately 18 degrees ([3]). The wedge half-angle is the angle between the chord line and the top or bottom surface of the leading edge of the vane, and for the simulation is equivalent to the impact angle at 0 degrees of vane rotation. Given material procurement constraints, the wedge half angle was bounded to an upper limit of 15 degrees. If the half-angle approaches 18 degrees, excessive erosion of the vane may occur, negatively affecting both the control and deflection of thrust. Conversely, with a shallower half-angle, there is the risk of insufficient surface area to direct the flow of the exhaust gas sufficiently. As a result, the wedge half-angle was chosen to be 10 degrees.

Since the vanes are immersed in a flow field with many complex levels of heat transfer, due to their direct exposure to exhaust gases and aluminum oxide particles, it is essential to understand the flow effects on the jet vanes for improved design and performance ([4]). CFD simulations and experimental studies are necessary to predict the flow effects of jet vanes, allowing for the refinement of jet vane geometries and materials in such conditions.

This paper is a result of testing and research from the GNC project within the Ramblin' Rocket Club at GT. It aims to provide a comprehensive understanding of the impacts of jet vanes on rocket propulsion dynamics through CFD analyses based on the commercially available Cesaroni Technology M1800-P motor. One goal of this study is to minimize heat transfer to the jet vanes and investigate erosion of the leading edge of the vanes under these conditions. Different geometry models were simulated in the motor exhaust flow, demonstrating the effect of leading-edge angle on erosion. Further flow dynamics simulations show the consequences of angle changes on thrust reduction. Vane materials for this project included tungsten carbide, copper-infused tungsten (CIT), and steel 4140 alloy. Cost, manufacturability, abrasion resistance, thermal conductivity, and service temperatures were considered for material selection. Overall, this project highlights the practical challenges and solutions associated with jet vane-based TVC systems and advances the field of active controls in amateur rocketry.

III. Simulation Methods

The jet vane analysis simulation methods address the primary design constraints and setup parameters for heat transfer, erosion rate, and thrust reduction. Simulations utilize CFD modeling for the flow of exhaust gases over the jet vanes. Similarly, erosion rate simulations focus on discrete-phase particle modeling, assessing factors such as particle size, velocity, and specific material properties to predict the erosion rate. Thrust reduction is calculated through an analysis of the exhaust flow up and downstream of the jet vanes. These simulation methods facilitate the refinement of the jet vane design, ensuring optimal performance.

A. Software Selection and Design Parameters

The primary software chosen for the CFD analyses was Ansys Fluent because of its robust turbulence models, high-performance solver, and wide scope of specialized capabilities for simulating reacting flows and heat transfer which make it well-suited for such an investigation.

These simulations modeled flow from the Cesaroni M1800-P solid rocket motor, which primarily uses ammonium-perchlorate composite propellant (APCP), a common propellant for hobby commercial-off-the-shelf (COTS) motors. Composite solid propellants use an oxidizer, a metal fuel for combustion stability and efficiency, a binder, a curing agent, a burn rate modifier, an explosive filler, a plasticizer, and an energetic plasticizer. For most hobby solid rocket motors, ammonium perchlorate is used as the oxidizer, hydroxyl-terminated polybutadiene is used as the binder, and solid aluminum powder is used as the metal fuel. The remaining chemicals are present in a much smaller percent composition and are considered negligible for erosion analysis. The vane material's erosion almost exclusively depends on the propellant's aluminum composition – the aluminum composition determines the corresponding aluminum oxide composition of the exhaust, which is the driving factor of unburned slag buildup and impact on the vanes. For simplicity purposes, a high mass percent of 20% was assumed for the aluminum oxide ([5]).

The vane geometry was created in SolidWorks, with a focus on accurately representing the fluid region and incorporating the negative area for the jet vanes. The initial geometry of the jet vanes was determined from prior precedent [1]. To properly simulate the environmental conditions downstream of the nozzle exit and the jet vanes, the ambient region was modeled with a diameter of 9 times the height of a jet vane and a depth of 10 times the length of a jet vane. The most accurate simulation geometry would model an environment with infinite radius and length, as there are no boundaries or walls restricting flow in real-world launch conditions. However, to minimize the computational effort taken on by Fluent, the environment was modeled using the aforementioned finite volume.

B. Simulation Setup Parameters

The simulation process begins by importing the SolidWorks model of the fluid geometry into Ansys Fluent with Fluent Meshing enabled. To define the specific boundary conditions, it is necessary to define their respective regions in the fluid geometry. These named selections are the faces of the inlet, outlet, nozzle wall, far-field wall, bounding wall, and jet vane walls. The vane walls were collectively defined as a single named selection as they would have the same region definitions. The next step of the simulation process is to mesh the fluid geometry. Meshing refers to the process of dividing a geometric model into a large number of small, finite-sized elements. Meshing applies the governing calculations and partial differential equations to each cell. Local sizing was chosen around the vane walls' named selection because of the increased accuracy and definition of the mesh geometry surrounding the vane walls. This refined mesh sizing allowed for the turbulent flow over the jet vanes to be modeled with a high degree of accuracy, in turn leading to better temperature and erosion estimates. A surface mesh was also constructed, breaking up the surface of the model geometry into its designated element sizes.

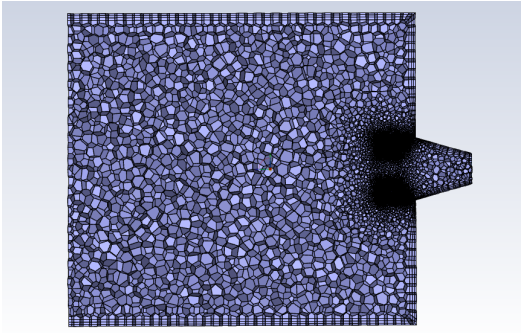


Fig. 1 Volumetric mesh cross-section with local sizing on jet vane faces

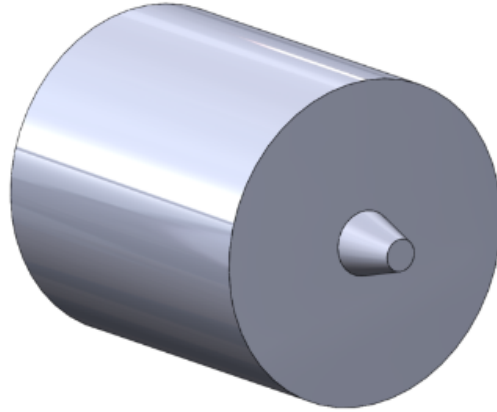


Fig. 2 Simulation Geometry

For this simulation, the mesh geometry consists of both fluid and void regions. The fluid regions are to be defined as the geometry's interior, while the void regions are the vanes themselves. The vanes are simulated as voids due to their state as cavities in the SolidWorks model.

The boundary conditions in the Fluent Meshing software are defined by assuming the nozzle to be ideal and isentropic, and flow was simulated from the throat of the nozzle to the end of the modeled ambient environment. This simplification was done to avoid simulating the nozzle flow and concentrate on the vanes themselves. The throat was considered to be a pressure inlet, and the static pressure, stagnation pressure, and static temperature were provided for this boundary condition. The static pressure and static temperature were found in the propellant data sheet. The stagnation pressure was calculated using Eq.(1).

$$\frac{p_t}{p} = \left(1 + \frac{\gamma - 1}{2} M^2\right)^{\frac{\gamma}{\gamma - 1}}. \quad (1)$$

For this simulation, Eq.(1) assumes M to be 1 because the flow is choked at the throat. The exit of the simulation geometry was considered a pressure outlet and assumed ambient pressure and ambient temperature. In the simulation setup, the outer surface, nozzle wall, and jet vanes were treated as boundary walls, assuming a no-slip shear condition. Additionally, the jet vanes were modeled using the thermal and mechanical properties of copper-infused tungsten to simulate realistic heat and stress responses during operation.

Table 1 A table of the boundary condition values.

Boundary Condition	Value
Pressure-Inlet Total Pressure	6904316 Pa
Pressure-Inlet Static Pressure	3847000 Pa
Pressure-Inlet Temperature	2356.583 K
Pressure-Outlet Gauge Pressure	101325 Pa
Pressure-Outlet Temperature	300 K
Gauge Pressure	0 Pa

C. Erosion Simulation

The two types of Fluent solvers are density-based and pressure-based. A density-based solver was used to model this simulation because the exhaust flow reaches Mach numbers greater than 3, requiring compressible flow calculations to simulate the shock waves over the jet vanes [6]. A pressure-based solver is later required to simulate the discrete phase particles for the calculation of the erosion rate of the jet vanes.

The solution models that Ansys Fluent requires to simulate the exhaust flow over the jet vanes are the energy equation and viscosity equation. The energy equation is necessary for the conservation of energy while the viscosity equation is necessary to determine the exchange of heat from the exhaust flow of the motor onto the jet vanes. For this simulation, the realizable $k-\epsilon$ model was used for turbulence. The $k-\epsilon$ model provides reasonable accuracy for a large range of turbulent flows, and is realizable, allowing for accurate predictions of the boundary layers under strong pressure gradients [6].

The exhaust flow of the motor was assumed to be air due to the lack of propellant chemistry information of the COTS motor. The air is simulated as an ideal gas, and the Sutherland equation model is used for air viscosity.

The material properties defined in this simulation relate the properties of density, specific heat, and thermal conductivity to each material. These properties allow for the accurate computation of energy transfer in the form of heat from the exhaust flow of gases over the jet vanes. For this simulation, copper-infused tungsten, tungsten-carbide, and steel-4140 were the three materials simulated as listed in table 2.

Table 2 Material properties for the chosen jet vane materials. ([7], [8], [9], [10], [11])

Property	Steel 4140	Copper-infused Tungsten	Tungsten Carbide
Density (kg/m^3)	7850	15700	14300
Heat Capacity (J/kg-K)	470	184	196
Thermal Conductivity (W/m-K)	52	88	190

Erosion of the jet vanes is simulated using Discrete Phase Modeling. Injections of inert aluminum solid particles are simulated, with a velocity vector normal to the inlet plane. Since a COTS motor is simulated, there is not enough data to accurately simulate the correct values of erosion. However, by keeping assumptions consistent across different simulations of the tested geometries, the proportion of erosion can be measured and compared. Aluminum solid particles are simulated instead of aluminum oxide particles as aluminum solid is the closest material choice available in Ansys Fluent to the desired aluminum oxide.

Multiple simulations can then be run with different vane geometries. The key dimensions to be analyzed for the jet vanes are the height and angle of the leading edge ???. The height of the jet vanes was chosen as 0.5 inches for ease of manufacturing and two different leading edge angles were tested: 50 degrees and 60 degrees. These angles generate a larger incidence angle of colliding particles, which reduces the erosion at the leading edge ([1]). Flow simulation and erosion analysis were tested at each angle and results were compared.

After finalizing the geometry of the jet vane, the center of pressure was calculated, as an ideal jet vane rotates about its center of pressure ([2]). The center of pressure is simulated separately, with a simplified bounding box that does not include the diverging nozzle. It is also assumed that the entire inlet wall uses the boundary conditions of the nozzle exit of the COTS motor. The pressure outlet is set at ambient conditions and the flow over the vane is simulated using the same models as before.

D. Thrust Reduction Calculations

The thrust reduction due to the vanes was calculated using Ansys CFD-post and the rocket thrust equation, shown in Eq.(2).

$$T = \dot{m}v + (P - P_a)A \quad (2)$$

Ansys CFD-post computed a 2-dimensional grid containing 1000 points in both x- and y-directions perpendicular to the direction of flow. By aligning this 2-dimensional grid with a plane set at the exit of the nozzle, the thrust, neglecting the reduction due to the jet vanes, can be found. Moving this plane further downstream of the jet vanes and finding the values of each point in the grid allows for the calculation of the thrust including the reduction from the jet vanes. Ansys CFD-post provides multiple different flow properties for the values of the grid, including density, pressure, and velocity. To calculate the mass flow rate, Eq.(3) is used.

$$\dot{m} = \rho v A \quad (3)$$

For each point in the grid, the product of the density and the velocity, or mass flux, was calculated. Multiplying the mass flux by the area associated with each point provides the mass flow rate. Since the grid was evenly divided, the area for each point was uniform, and by choosing a large number of points, the accuracy of the overall thrust calculation was improved. The mass flow rate was then substituted into Eq.(2) and multiplied by the velocity associated with each area shown. The second term of Eq.(2), the force due to pressure, was calculated by subtracting the ambient pressure from the local pressure at each point in the grid and multiplying this term by the area associated with each element. Finally, adding the pressure force to the first term and summing the values for each element provides the overall thrust through a single plane. The percent thrust loss was calculated using Eq. (4).

$$\text{Thrust Reduction} = \left(1 - \frac{T_{\text{vanes}}}{T_{\text{true}}}\right) * 100 \quad (4)$$

IV. Results and Discussion

A. Flow Around Singular Jet Vane

After finalizing the geometry of the jet vane, the flow dynamics around a singular vane were simulated using a simple cylindrical geometry with a single vane centered in the middle. The inlet boundary condition was the nozzle exit flow properties and the outlet condition was the ambient environment properties.

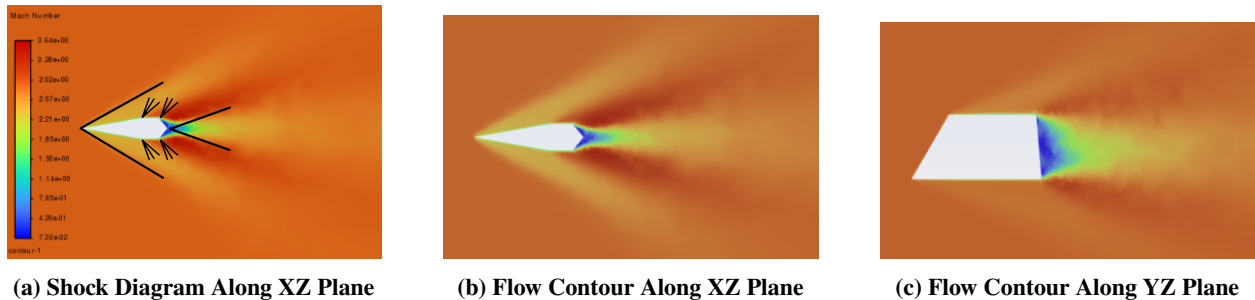


Fig. 3 The flow visualized around a single jet vane using nozzle exit conditions.

The initial design of the jet vane was created with a supersonic airfoil that featured a sharp leading edge to minimize wave drag ([12]). The airfoil forms a diamond shape that maintains a greater lift-to-drag ratio during the large angular rotation of the jet vanes. This airfoil shape creates shocks and expansion fans instead of forming boundary layers. These flow formations are evident in Fig. 3 and provide reasonable verification of the chosen vane geometry.

B. Heat Transfer Analysis

The heat transfer simulated for three different materials is presented in Fig. 4. The maximum value of heat is expected to occur at the back of the vanes where the flow loses the largest amount of kinetic energy due to the oblique

shocks. The heat transfer is the greatest for steel-4140, followed by tungsten-carbide and finally copper-infused tungsten. Using these temperature contours, the best material for the jet vanes would be copper-infused tungsten.

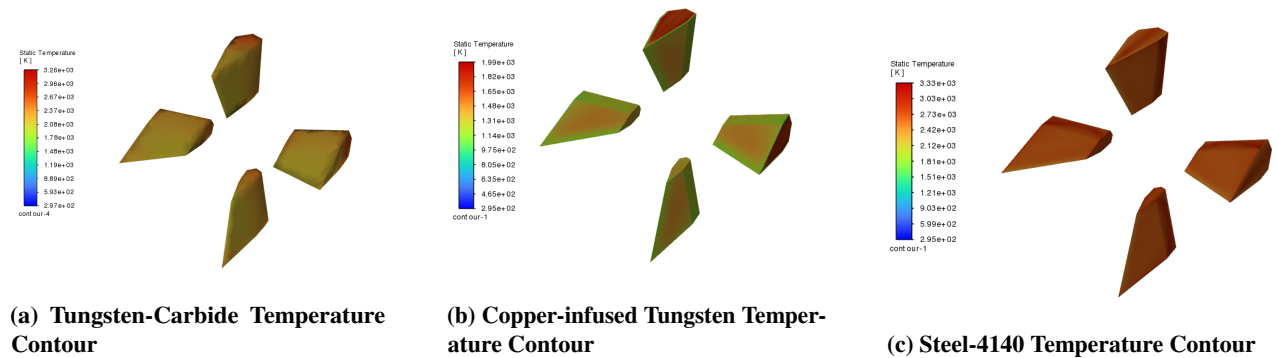


Fig. 4 The temperature contours for the different materials selected

C. Erosion Analysis

Erosion of the jet vanes was simulated at 50 degrees and 60 degrees. Fig. 5 displays the rate of erosion steadily increasing as the angle of the leading edge increases.

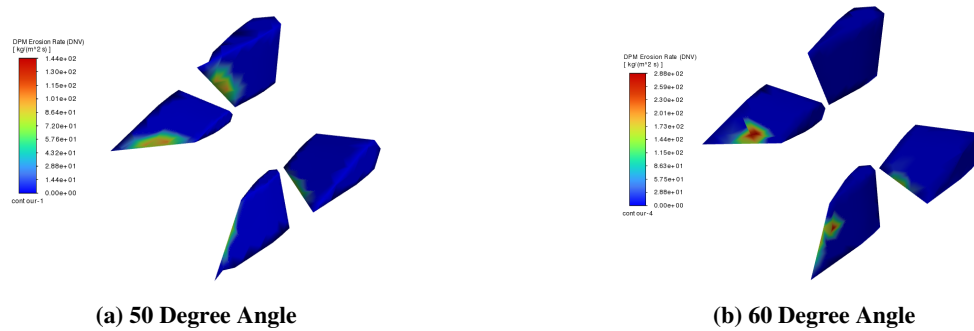


Fig. 5 The flow visualized around a single jet vane using nozzle exit conditions.

In erosion analysis for the vanes, the leading edge angle is crucial to determining the amount of abrasion on the surfaces exposed to the COTS motor's exhaust flow. The erosion rates at two different leading-edge angles were assessed, and Fig. 5 illustrates this relation. The erosion rate is lowest at a leading-edge angle of 50 degrees, making it the most optimal selection for vane geometry. Simulations following this use the 50-degree leading edge angle for their vane geometry.

D. Location of the Center of Pressure

Using the high-fidelity simulation described in IV.A, the team found the center of pressure of the jet vane in the plane coincident with the root chord. The location along the chord of the center of pressure was used in IV.F to rotate 2 opposing jet vanes about the axis going through their center of pressure, shown in Fig. 6.

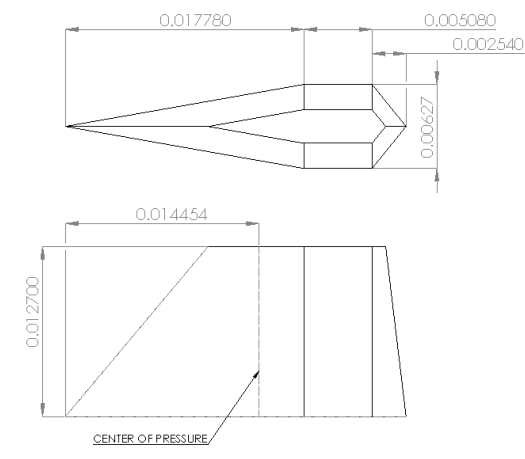
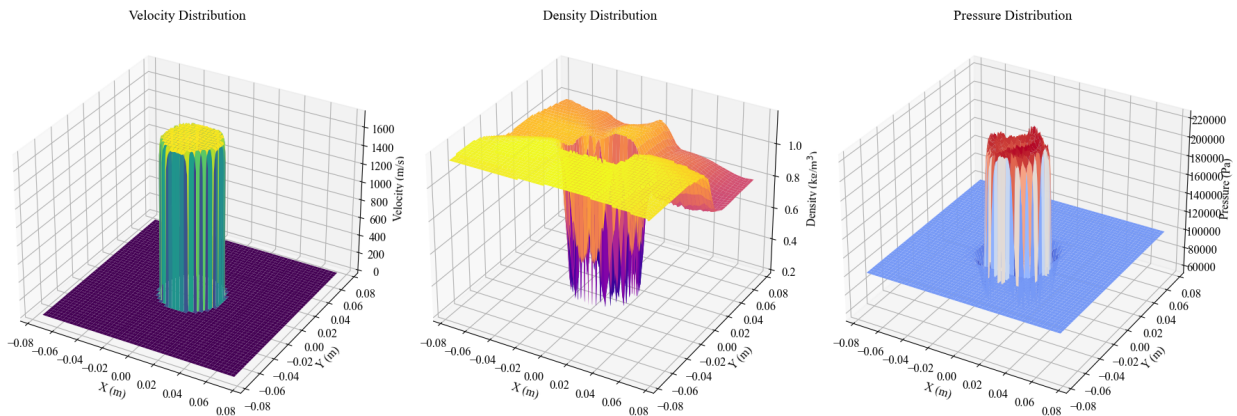


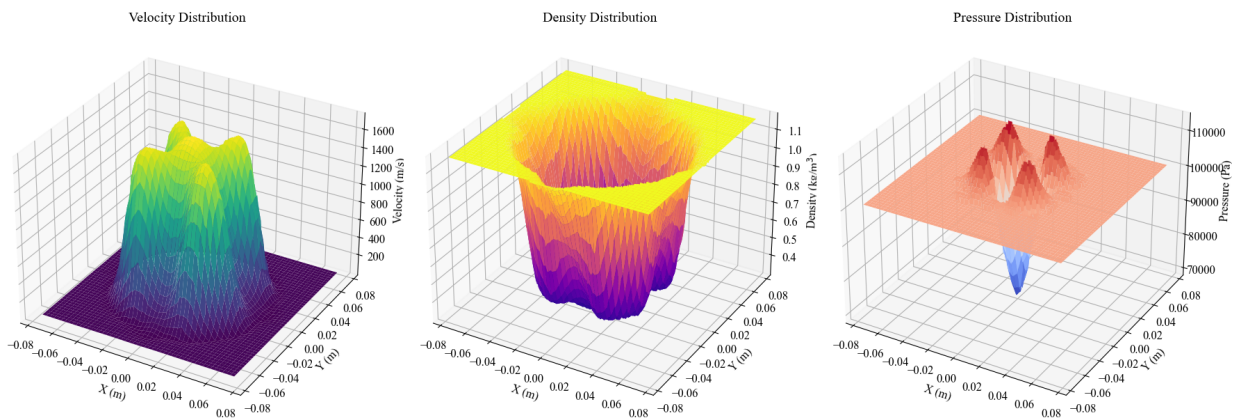
Fig. 6 The location of the center of pressure along the chord of a single vane.

E. Thrust Reduction

Using the process outlined in III.D, the density, velocity, and pressure were found at each point in each plane. Figure 7 displays the 3-dimensional contours of these flow properties.



(a) The density, velocity, and pressure at the exit plane of the nozzle.



(b) The density, velocity, and pressure downstream of the jet vanes.

Fig. 7 The flow properties at the exit plane of the nozzle and the plane further downstream of the jet vanes.

Given the values for the plots and following the aforementioned procedure, the thrust at each plane and thrust reduction could be calculated. These values are shown in table 3.

Table 3 Thrust performance of vanes.

Property	Value
T_{vanes}	3829.40 N
T_{true}	3985.19 N
Thrust Reduction	3.9093%

The low percentage of thrust reduction validates the proposed vane design, as it indicates a relatively low amount of energy loss. A further decrease in thrust would complicate control, as lowered thrust decreases TVC effectiveness.

F. Jet Vane Thrust Vectoring

As previously described in IV.D, two vanes were rotated around their centers of pressure at various angles to observe the effects on the overall thrust vector. These simulations ran for vane rotations of 0° , 10° , 20° , and 30° . As demonstrated in Fig. 8, Fig. 9, Fig. 10, and Fig. 11, the vane rotation is directly correlated to the angle of the exhaust flow velocity.

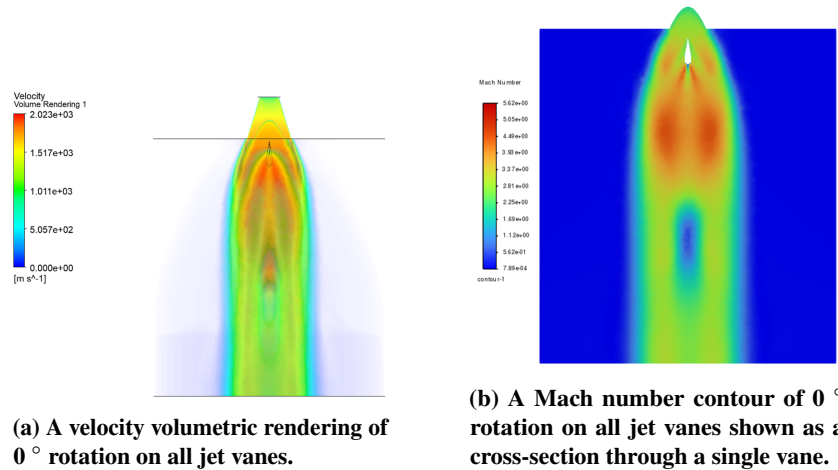
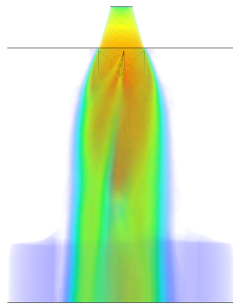
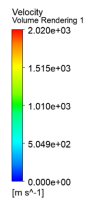
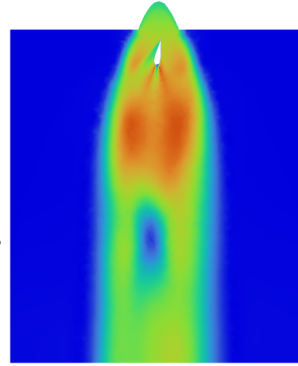
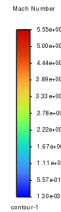


Fig. 8 Volumetric rendering and Mach number contours displayed for 0° rotation.



(a) A velocity volumetric rendering of 10° rotation on two jet vanes on opposite sides.

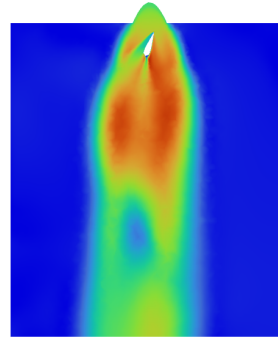
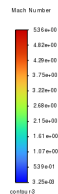


(b) A Mach number contour of 10° rotation on two jet vanes shown as a cross-section through a single vane.

Fig. 9 Volumetric rendering and Mach number contours displayed for 10° rotation.

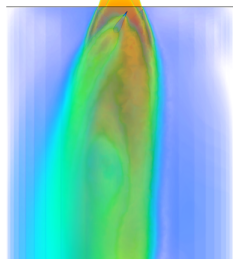
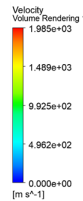


(a) A velocity volumetric rendering of 20° rotation on two jet vanes on opposite sides.

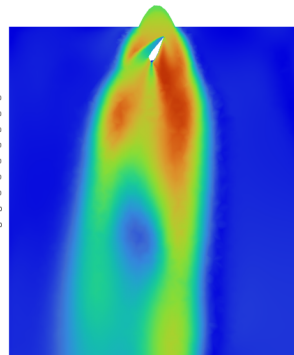
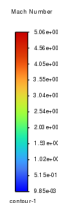


(b) A Mach number contour of 20° rotation on two jet vanes shown as a cross-section through a single vane.

Fig. 10 Volumetric rendering and Mach number contours displayed for 20° rotation.



(a) A velocity volumetric rendering of 30° rotation on two jet vanes on opposite sides.



(b) A Mach number contour of 30° rotation on two jet vanes shown as a cross-section through a single vane.

Fig. 11 Volumetric rendering and Mach number contours displayed for 30° rotation.

By extension, the velocity volumetric renders in Fig. 8, Fig. 9, Fig. 10, and Fig. 11, show a change in the visible thrust vector angle as a function of the vane rotation. These results validate prior design choices as they demonstrate the current jet vane design is capable of altering the direction of thrust.

V. Conclusion

This paper utilizes CFD simulations to research various design parameters for a JVTVC system, namely theoretical heat transfer across different materials, erosion across different geometries, and thrust reduction. By finding the temperature contours of the vanes in the flow, the team determined that CIT was the best material for the vanes due to its comparatively low temperature at the leading edge. The team also investigated the effects of the leading edge's angle on flow properties, demonstrating that the 50-degree leading edge had the lowest erosion rate. This result validates that increasing the angle of the leading edge reduces the erosion rate on the jet vanes. With the 3.9% thrust reduction, the aerodynamic drag induced by the jet vanes is minimal and comparably lower than the average 6% thrust reduction.

Software and available data resources are limiting factors in the accuracy of the simulation results. Boundary condition assumptions such as exhaust flow plane initial velocity and far-field location were made by the team due to the unavailability of nozzle data from Cesaroni and computational power. Simulation accuracy was also limited by a relative lack of propellant data, which would affect exhaust flow properties. Since the exact aluminum oxide content of the propellant is unknown, the true concentration could invalidate the observed erosion. While the metrics used for the results rely on relative proportions rather than magnitudes to compare values across different materials, these are still notable considerations for future simulations.

The simulations provide a framework for jet vane design regarding leading edge angle and material selection. Furthermore, the simulations characterized the redirection of thrust at various angles of attack. To validate these results, the team is developing a test stand capable of producing and measuring pitch, roll, and yaw moments caused by the jet vanes. After validating the simulations, the team plans to develop an actively stabilized JVTVC rocket.

Acknowledgments

The authors wish to extend their gratitude to the Ramblin' Rocket Club at the Georgia Institute of Technology for the support and resources provided.

References

- [1] Josef Biberstein, S. K., Ezra Tal, "Thrust Vectoring of Small-scale Solid Rocket Motors Using Additively Manufactured Jet Vanes," Tech. rep., Massachusetts Institute of Technology, 2021.
- [2] Sobering, J. G., "Design and characterization of a thrust vane position controller for exhaust flow deflection TVC with dynamically changing loads," 2018.
- [3] Magnee, A., "Generalized law of erosion: application to various alloys and intermetallics," Tech. rep., Centre de Recherches Metallurgiques and University of Liege, Department of Applied Sciences, Metallurgy and Materials Science, 1994.
- [4] NUNN, R., and CA, N. P. S. M., "TVC (Thrust Vector Control) Jet Vane Thermal Modeling Using Parametric System Identification," 1988.
- [5] Lysien, S. A. . J. T., K., "Solid Propellant Formulations: A Review of Recent Progress and Utilized Components," Tech. rep., Department of Physical Chemistry and Technology of Polymers, Silesian University of Technology., 2021.
- [6] ANSYS, "ANSYS FLUENT 12.0 Theory Guide," *ANSYS FLUENT 12.0/12.1 Documentation*, 2024.
- [7] "AISI 4140," <http://www.matweb.com/search/DataSheet.aspx?MatGUID=8b43d8b59e4140b88ef666336ba7371a&ckck=1>, 2024. Accessed: 2024-03-03.
- [8] "Properties: Tungsten carbide - an overview," <https://www.azom.com/properties.aspx?ArticleID=1203>, 2024.
- [9] "Data sheet tungsten-copper (WCU)," <https://www.whs-sondermetalle.de/images/pdf/WCu-Tungsten-Copper.pdf>, 2024.
- [10] "Tungsten Carbide, WC," <https://www.matweb.com/search/DataSheet.aspx?MatGUID=e68b647b86104478a32012cbbd5ad3ea>, 2024.

[11] “4140 low-alloy steel,” <https://www.desktopmetal.com/uploads/SPJ-SPC-MDS-4140-210602.c.pdf>, 2024.

[12] Leishman, J. G., “INTRODUCTION TO AEROSPACE FLIGHT VEHICLES,” Tech. rep., Embry-Riddle Aeronautical University, 2024.